Int. J. Electrochem. Sci., 17 **(2022)** Article Number: 220520, doi: 10.20964/2022.05.03

International Journal of
ELECTROCHEMICAL
SCIENCE
www.electrochemsci.org

Simulated Annealing ANN Approach for Parameter Optimization of Micro-scaled Flow Channels Formation by Electrochemical Machining

Feng Ji[1,2,*], *Byungwon Min*[1,*]

[1] School of Engineering, Mokwon University, Daejeon 35349, Republic of Korea
[2] School of Xinglin, Nantong University, Nantong 226000, P. R. China
[*]E-mail: iems@ntu.edu.cn; minfam@mokwon.ac.kr

Received: 20 January 2022 / *Accepted:* 25 February 2022 / *Published:* 5 April 2022

In this paper, an artificial neural network based on simulated annealing was constructed. The mapping relationship between the micro-scaled flow channels' electrochemical machining parameters and the shape of the channel was established by training the samples. The depth and width of micro-scaled flow channels electrochemical machining on stainless steel surface were predicted, and the flow channels experiment was carried out with pulse power supply in $NaNO_3$ solution to verify the established network model. The results show that the depth and width of the channel predicted by the simulated annealing artificial neural network with a "4-7-2" structure are very close to the experimental values, and the error is less than 5.3%. The predicted and experimental data show that the etching degree in the process of channel electrochemical machining is closely related to voltage and current density. When the voltage is less than 5V, a "small island" is formed in the channel; When the voltage is greater than 40V, the lateral etching of the channel is relatively large, and the "dam" between the channels disappear. When the voltage is 25V, the machining morphology of the channel is the best.

Keywords: micro-scaled flow channel; neural network; simulated annealing; electrochemical machining; prediction model; parameter optimization

1. INTRODUCTION

Electrochemical machining（ECM）is based on the principle of electrochemical anodic dissolution. The cathode "tool" is not in direct contact with the workpiece, and has no effect of "cutting force" and "cutting heat". There will be no residual stress on the workpiece surface and recast layer like laser machining. It can process metal materials which is difficult to cut, such as stainless steel, quenched steel, and alloy. It has been continuously developed and applied in the processing of aero-engine blades、guns、gun barrel rifling and other parts [1-3]. Based on the regression model, Aakash et al. [4]

predicted the material removal rate and surface roughness in nickel base alloy ECM, and optimized the process parameters such as voltage, electrode gap, and prop feed speed. The predicted results are helpful to improve the production capacity. Farwaha et al. [5] studied ultrasonic-assisted electrochemical magnetic grinding by topsis method, calculated the influence of processing time, voltage, frequency, and other parameters on workpiece forming results with the mathematical model, and verified the rationality of the calculation results by 27 groups of experiments. Tsai et al. [6] studied the influence of parameters such as voltage and mask thickness in the mask through the Taguchi method. The machining test of the elliptical workpiece was carried out by taking red copper as a tool, stainless steel(SUS304) plate as a workpiece, and electrolyte lateral flow as the condition. It was concluded that the main parameters affecting the machining results are the aperture and thickness of the mask.

Malik et al. [7] used the grey correlation analysis method to predict the laser-assisted machining of conical holes. Through the optimal combination of parameters, the machining time was shortened. It was found that when the power supply voltage was 80V, the electrolyte concentration was 40 g/*l*, the gap between electrodes was 3mm and the duty cycle was 60%, the maximum material removal rate (MRR) increased by 29.16%, and the surface roughness decreased by 36.83%. Antil et al. [8] used a Genetic algorithm to study the fiber residue of polymer matrix composites in the process of micro-drilling. Taking voltage, electrolyte concentration, and duty cycle as process parameters, the MRR and taper are obtained by regression analysis, which solves the problem of the high costs of ECM experiments for composite materials.

Fang et al. [9] proposed an optimization method based on the iterative solution of the multi-physical model, which solved the complex problem of cathode optimization design in pulse electrochemical machining (PECM), and introduced a multi-physical field model to describe the influence of pulse parameters on electrolyte conductivity distribution reflecting gap distribution, the accuracy of cathode shape forming is improved. Das et al. [10] used an ant colony algorithm to find the optimal combination of MRR and minimum surface roughness (SR) parameters in the electrochemical machining of steel. Vikas et al. [11] tried to optimize the MRR and SR in ECM by a Genetic algorithm. The combined parameters of the genetic algorithm were obtained by the response surface method, but they need to be based on all parameters in early processing, which has certain limitations. Pang et al. [12] used a backpropagation neural network to establish the complex nonlinear relationship between process parameters and workpiece surface roughness and obtained the optimal configuration of processing parameters that can make the surface roughness parameters change greatly. The experimental results show that the error of the prediction result is 0.1, and the prediction accuracy of roughness needs to be further improved. Li et al. [13] used an artificial neural network to evaluate and optimize parameters of aero-engine blade machining: voltage, initial machining gap, cathode feed rate, electrolyte temperature, and electrolyte inlet and outlet pressure difference. The optimized parameters meet the machining requirements of blades and have good electrochemical machining stability, However, the generalization ability of the trained neural network is weak and can not be transplanted to micro-scaled flow channels machining.

Song et al. [14] used a deep neural network to predict the thermal and residual stresses in the electrochemical machining of nickel-titanium alloy, but limited to the premise of constant given temperature, through the evaluation of root mean square error, better results were obtained than the

regression method. The experiment depends on a large amount of data, but conventional ECM does not have a large-scale database, which limits the applicability of this method in micro-scaled flow channels machining. Kasdekar et al. [15] established a multilayer perceptron model with a backpropagation algorithm and selected process parameters such as voltage, feed rate, electrolyte concentration, and electrode (Cu) as inputs. The model has certain results in predicting the anode dissolution rate.

Lu et al. [16] proposed a new method to predict the borehole diameter in ECM by using a bayesian optimized depth convolution network. Using feed rate, pulse time, and voltage as input parameters, the training speed and accuracy are improved compared with the traditional neural network.

Manoochehri et al.[17] used ANN of simulated annealing to model and optimize the drawing process of 304 stainless steel (SUS304). The die radius, punch radius, blank holder force, and friction conditions were selected as input parameters. As one of the main failure modes of deep drawing parts, thinning is considered as the process output parameter. By selecting appropriate process parameters, the purpose of uniform wall thickness and minimum thinning can be realized.

Generally, researchers are trying to improve the traditional ECM experimental method with various methods and strive to find the best machining process parameters, such as genetic algorithm, ant colony algorithm, regression model, neural network, and deep learning, which have achieved good results. However, the above methods are limited to the micro-scaled flow channels ECM concerned in this paper. Therefore, a backpropagation neural network based on a simulated annealing algorithm is constructed in this paper to find the optimal parameters of micro-scaled flow channels machining on the stainless steel surface.

The remainder of the paper is structured as follows. Section 2 provides details about the electrochemical machining method, backpropagation neural network method, and artificial neural network method based on simulated annealing algorithm. The network prediction results and test results are given in Section 3 and the paper ends with a conclusion in Section 4.

2. METHODS

2.1. Electrochemical machining method

As shown in Figure1, the self-developed micro-scaled flow channels ECM system is included an electrolyte circulation system, a metal double-layer fixture system, and a power control system. The internal area of the metal double-layer fixture system is made of plexiglass material, with good overall sealing and corrosion resistance, which is easy to be fixed on marble. The electrolyte inside the double-layer fixture adopts the flow measurement method. The electrolyte flows through the flow channel with gentle cross-section change, and the speed and pressure change slowly. The flow field uniformity is good, which can prevent cavitation and is conducive to the design and forming of anode workpiece. The distance between anode and cathode is fixed at 4mm. The electrolysis control system adopts the single pulse power supply of rsnp-4050, which is more reliable than the general DC power supply.

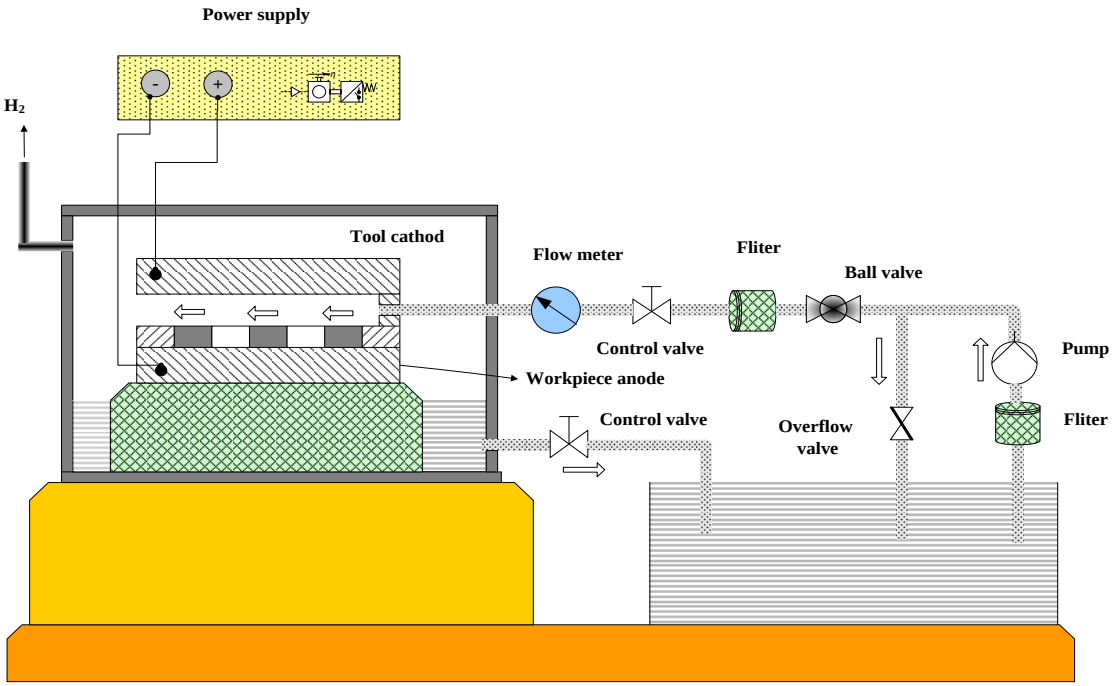

Figure 1. Micro-scaled flow channels ECM system

The electrolyte adopts $NaNO_3$ aqueous solution, which has little effect on hydrogen evolution, and the surface with roughness R_a 0.32 can be obtained. The reaction temperature during ECM is controlled between 28-32℃. The configuration of the pulse power supply and other parameters in the ECM system is shown in Table 1.

Table 1. Parameter configuration of ECM system.

System name	Content or parameter
$NaNO_3$ electrolyte（*mol/L*）	10%
Electrolyte temperature（*℃*）	28-32
The output voltage of pulse power supply（*V*）	10-40
The output current of pulse power supply（*A*）	0-50
Duty cycle（*%*）	30-70
Frequency（*kHz*）	0.5,1,2,3

According to Faraday's first law and second law, the volume V of anodic dissolved metal is described by the following Equation(1):

$$V = \frac{M}{\rho} = \frac{KIt}{\rho} \quad (1)$$

The micro-scaled flow channels depth d_m is described by the following Equation(2):

$$d_m = \frac{V}{S} = \frac{KIt}{\rho S} = \frac{KDt}{\rho} \quad (2)$$

In Equation (1-2), ρ is the metal density (g/cm3), I is the circulating current (a), t is the current flow time (s), D is the current density, s is the dissolved bottom area of the anode workpiece channel (dm^2).

The frequency *f* and duty cycle *PD* of the pulse power supply directly affect the corrosion depth and surface roughness of the workpiece processing. The pulse power supply changes in a pulsed manner, causing the electrolyte pressure fluctuation in the processing gap and disturbing the electrolyte. When *f* reaches 1kHz and $PD \leq 0.5$, it can strengthen and homogenize the flow field, reduce polarization, improve the anodic dissolution and reduce the surface roughness of the flow channels. Figure 2 shows a picture of the test results of electrochemical machining of short micro-scaled flow channels with $NaNO_3$ electrolyte.

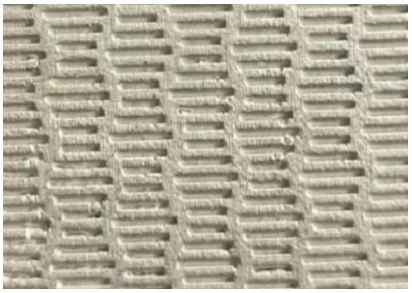

Figure 2. Image of short micro-scaled flow channels.

Therefore, this research aims to establish a nonlinear mapping model between the parameters (voltage, current density, pulse frequency, and pulse duty cycle) and micro-scaled flow channels (depth and channel width).

2.2 Artificial neural network model.

2.2.1 Model design

In this paper, a backpropagation neural network is used to predict the channel depth and channel width of micro-scaled flow channels ECM. It is a multilayer feedforward network composed of the input layer, hidden layer, and output layer. The input and output parameter selection method in literature [7] [8] [13] [15] [17] is used as a reference for this research. In the optimization of micro-scaled flow channels ECM, four factors affecting channels forming are selected as the inputs of the neural network, including current density *D*, pulse frequency *f*, voltage *U* and pulse duty cycle *PD*. The four components correspond to the input layer nodes respectively, and each generation represents an influencing parameter, which has different physical significance, the output terms of the artificial network are the depth d_m and width w_m of the flow channels.

In this research, the trial and error method [18] and Kolmogorov theorem [19] were combined to determine the number of the hidden layer nodes. Firstly, the nodes number is determined by equation (3) and then corrected according to the Kolmogorov theorem. It is determined that the performance is the best when there are 7 nodes. The network structure is shown in Figure 3.

$$m = \sqrt{n + l} + c \quad (3)$$

In Equation (3), *m* is the number of the hidden layer nodes, *n* is the number of the input layer nodes, ***l*** is the number of the output layer nodes, $c \in [1,10]$.

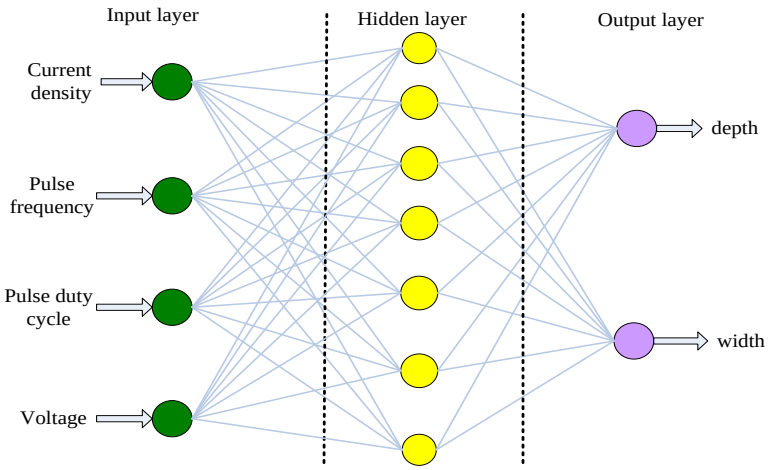

Figure 3. Artificial neural network structure.

2.2.2 Variables and training of ANN

In this paper, the variables and parameters of ANN were defined, as shown in Table 2. The transfer function in the ANN model training is the unipolar sigmoid function, which makes the neural network have better approximation and generalization ability in the ECM of micro-scaled flow channels.

Table 2. Meaning of symbols.

Symbol	Meaning	Symbol	Meaning
X	Input layer vector	y_j	Output of h
O	Output layer vector	δ_j^h	Error signal of h
d	Output layer expectation vector	δ_k^o	Error signal of the output layer
V_{ij}	Weight between input layer and h	ε	Accuracy of network
W_{jk}	Weight between h and output layer	η	Learning rate
h	A layer of hidden layer	b	Threshold
p	Sample counter	q	Training times counter

The value of the output layer in the neural network is calculated by Equation (4):

$$O_k = f(\sum_{j=0}^{m} w_{jk}\, y_j + b) \tag{4}$$

In Equation (4), f is the transfer function, m is the number of neurons in the hidden layer, and b is the threshold of the transfer function f. f is a continuous and differentiable nonlinear function, expressed by Equation (5):

$$f(x) = (1 + e^{-x})^{-1} \tag{5}$$

The artificial neural network adjusts the network through error backpropagation so that the global error of the network decreases continuously and finally tends to the convergence threshold. The error of each layer in the network is the difference between the actual network output and the expected output. The error of the output layer is calculated by Equation (6):

$$E^o = \frac{1}{2}(d-o)^2 = \frac{1}{2}\sum_{k=1}^{l}(d_k - o_k)^2 \quad (6)$$

The error of the hidden layer is calculated by Equation (7):

$$E^h = \frac{1}{2}\sum_{k=1}^{l}[d_k - f(\sum_{j=0}^{m} w_{jk}\, y_j + b)]^2 \quad (7)$$

The error of the input layer is calculated by Equation (8):

$$E^h = \frac{1}{2}\sum_{k=1}^{l}\{[d_k - f(\sum_{j=0}^{m} w_{jk}\, f(\sum_{j=0}^{n} v_{ij}\, x_i)]\}^2 \quad (8)$$

The influence of the weight of each layer of ANN is the main cause of the error in the network. The error is changed by adjusting the weight of each layer. In this paper, an error signal is defined for the output layer and the hidden layer respectively, which is calculated by Equation (9-10):

$$\delta_k^o = (d_k - o_k)o_k(1-o_k) \quad (9)$$

$$\delta_j^y = -\frac{\partial E^h}{\partial \sum_{j=0}^{n} v_{ij}\, x_i} = \sum_{k=1}^{l}\delta_k^o w_{jk} y_i (1-y_j) \quad (10)$$

The error signal of each layer in Equation (9-10) is used to adjust the weight of the corresponding network layer. In this paper, the learning rate is defined as η, and weight adjustment is calculated by Equation (11) (12):

$$\Delta w_{jk} = \eta\delta_k^o y_j = \eta(d_k - o_k)o_k(1-o_k)y_j \quad (11)$$

$$\Delta v_{ij} = \eta\delta_j^y x_i = \eta(\sum_{k=1}^{l}\delta_k^o\, w_{jk})y_j(1-y_j)x_i \quad (12)$$

In this paper, the training algorithm of the neural network prediction model for micro-scaled flow channels ECM was designed, the algorithm is shown in Table 3:

Table 3. Training algorithm of ANN model for micro-scaled flow channel ECM.

Algorithm1: ANN Training Algorithm
Input: Sample set; Counter ***p***; Training times counter ***q***; Weight matrix ***W***, ***V***; Learning rate $\boldsymbol{\eta}$; Error accuracy $\boldsymbol{\varepsilon}$ =10^{-4}.
Output: Trained ANN prediction model().
1. Initialization ***p, q,*** **W, V,** $\boldsymbol{\eta}$, ε
2. **For**(int *i*; E^O>ε;i++)
3. {
4. **Do** {
5. Input Sample set();
6. Calculate $\boldsymbol{o_k}$, $\boldsymbol{y_i}$ with Equation (4-5);

```
7.          Calculate E^o, E^p, E^in with Equation (6-8);
8.          Calculate error signal δ with Equation (9-10);
9.          Adjust the w_jk, v_ij with Equation (11-12); }
10.       While(p<P)
11.       }
12.         Output Trained ANN prediction model ();
13.       End
```

In the process of adjusting the network weight and threshold, the error in each layer of the network can be reduced only in the direction that can be reduced. This way of error reduction may lead to the local optimal solution in the process of error reduction.

To avoid this problem, the ANN is optimized based on a simulated annealing（SA） algorithm. The energy in the SA algorithm can change in different directions with the help of the random disturbance mechanism and Metropolis criterion, to jump out of the local energy minimum. Next, the optimized SA-ANN model is described.

2.3 Optimization of ANN-based on Simulated Annealing

A simulated annealing algorithm was established by the metropolis. When updating the feasible solution, it aims to jump out of the local optimal solution, to achieve global optimization. According to the Metropolis criterion, when the temperature is T, the probability of cooling with energy difference ΔE is calculated by Equation (13) :

$$\boldsymbol{p(dE) = exp(-\frac{\Delta E}{kT})} \tag{13}$$

Where k is the Boltzmann constant and exp is the natural index, $\Delta E < 0$, $\Delta E/kT < 0$, $p(dE) \in (0,1)$. The larger T, the cooling probability of energy difference ΔE is greater; The smaller T, the cooling probability is smaller.

If the objective function is $f(x)$, the initial temperature is T_0, the lower temperature limit is T_{min}, the current feasible solution is $\boldsymbol{x}$, the new solution after iteration is x_{new}, and the energy difference is defined as $\Delta f = f(x_{new})-f(x)$.

If $\Delta f < 0$, x_{new} is accepted as the new current solution; otherwise, the probability $exp(-\Delta f/kT)$ accept x_{new} as the new current solution, cool down slowly after meeting the number of iterations, reset the number of iterations, and finally output the optimal x_{new} when $t=T_{min}$.

In this paper, the perturbation model for generating new solutions is to be improved. The improved model is applied in finding the minimum of the error function. The algorithm is shown in Table 4. The error function E^o in ANN is selected as the objective function, x as the comprehensive vector connecting weights V_{ij}, W_{jk}, and threshold b in ANN, and the random disturbance generation model is defined as $x_{new} = x+\alpha\times(t/L)\times Rand$, α as the disturbance amplitude parameter, t/L representing the ratio of the current temperature to the maximum of iterations, and $Rand$ generates random numbers between (-1,1), to realize optimization.

Table 4. Simulated annealing artificial neural network training algorithm.

Algorithm1: SA-ANN training algorithm	
Input: Initial temperature $\boldsymbol{T}$; Lower temperature limit $\boldsymbol{T_{min}}$; Initial solution state $\boldsymbol{x}$; Number of iterations per T value $\boldsymbol{L}$.	
Output: $\boldsymbol{x_{new}}$， $\boldsymbol{E}(\boldsymbol{x_{new}})$, Trained SA-ANN prediction model().	
1.	Initialization $\boldsymbol{T}$, $\boldsymbol{T_{min}}$, $\boldsymbol{x}$, $\boldsymbol{L}$
2.	**Call** BP($\boldsymbol{w},\boldsymbol{v},\boldsymbol{b}$)→$\boldsymbol{x}$， $f(x)=E^o(x)$
3.	**For** ($\boldsymbol{T}$; $\boldsymbol{T}>\boldsymbol{T_{min}}$; i++)
4.	{
5.	**Do** {
6.	According to $\boldsymbol{x_{new}}=\boldsymbol{x}+\Delta\boldsymbol{x}$, Calculate $\boldsymbol{x_{new}}$, $\Delta\boldsymbol{x}$ is the random value between d_{min} and d_{max}
7.	**Get** BP ($\Delta\boldsymbol{w}$, $\Delta\boldsymbol{v}$, $\boldsymbol{b}$), calculate the error function: $\boldsymbol{E}(\boldsymbol{x_{new}})$
8.	Based on $f(x)$, calculate$\Delta\boldsymbol{E}=\boldsymbol{E}(\mathbf{x_{new}})-\boldsymbol{E}(\mathbf{x})$
1.	**If** ($\Delta\boldsymbol{E}$<=**0**)
2.	**then** $\boldsymbol{x}=\boldsymbol{x_{new}}$, $\boldsymbol{E}(\boldsymbol{x})=\boldsymbol{E}(\boldsymbol{x_{new}})$
3.	**Else**
4.	According to probability **exp**(-$\Delta\boldsymbol{E}/\boldsymbol{kT}$) accept $\boldsymbol{x_{new}}$ as a new solution
5.	$\boldsymbol{l}$++}
6.	**Until**($l=L$)
7.	$\boldsymbol{T}=\boldsymbol{\lambda}\ \boldsymbol{T}$
16.	}
17.	**Get**($\boldsymbol{x_{new}}$)→ANN Training($\boldsymbol{W},\boldsymbol{V}$)
18.	**End**

In this paper, the SA-ANN training algorithm constructed in Table 4 is used to train the neural network model. After the model training reaches the prediction accuracy, it can be used to predict the channel processing parameters.

3. RESULTS AND ANALYSIS

3.1. Sample Pretreatment

Firstly, the samples were screened, and some samples are shown in Table 5. Then the sample data were normalized to avoid the saturation of neuron output caused by too large value and affect the convergence speed. In this paper, it was normalized with Equation (14).

$$x^* = \frac{x - x_{min}}{x_{max} - x_{min}} \tag{1}$$

x* is the normalized value, x is the original value, x_{min} is the minimum value in the sample, and x_{max} is the maximum value in the sample.

Table 5. Partial sample.

Name	Import				Teacher	
	D/A·dm^{-2}	f/kHz	PD/%	U/v	d_m/μm	w_m/μm
1	14	2	40	10	152.88	334.50
2	16	2	40	20	160.25	362.25
3	18	2	40	30	190.43	384.34
4	24	2	40	40	231.16	290.93
5	28	1.5	40	45	152.88	334.50

3.2 Analysis of Network Model Experiment Results

In this paper, the nodes number in the hidden layer of ANN and SA-ANN was evaluated, the impact of a different nodes number in the hidden layer on the network performance was detected through the same sample, the nodes number was selected when it has the smallest relative error of the prediction result, and the relative error of the network is less than 0.08. Compared with the literature [12], the error rate is reduced by 0.02. The optimal structure of the single hidden layer network was determined as 4-7-2. The hidden layer has seven nodes. Which had a good effect on network prediction. The results of the experiments are shown in Table 6.

Table 6. Network performance with a different number of neurons.

Number of nodes in the hidden layer	ANN Relative Error	SA-ANN Relative Error
9	0.133	0.102
8	0.098	0.085
7	0.075	0.053
6	0.089	0.079
5	0.112	0.093
4	0.129	0.109

3.3. Model Prediction Results

The trained SA-ANN prediction model was used to predict the results of micro-scaled flow channels ECM, and the process parameters were used as the input of the neural network to predict the results of stainless steel micro-scaled flow channels ECM. The output value of the neural network and the actual electrolysis results of the experiment are shown in Table 7. The current density values were 12A,15A, 19A, 22A, and 28A, the pulse frequency values were 0.5kHz, 1.5kHz, and 2kHz, the pulse duty cycle values were 40% and 60%, the output parameters comply with the law of actual processing, and the depth of micro-scaled flow channels was between 24.181~151.273μm, the width of flow channels was between 169.761~353.723μm, the depth and width of the flow channels vary significantly with the voltage and current density. The pulse size directly affected the processing time.

In Table 7, the error between the predicted value and the actual value of the micro-scaled flow channel ECM was small, and the predicted value of the network was less than 5.3%. Compared with the literature [7][8][12], the prediction accuracy is better in this research. The experimental data show that the neural network based on simulated annealing had good generalization ability.

Table 7. The comparison of SA-ANN prediction with experimental results.

Name	Network Input				Network Output		Experiment Results	
	D/A·dm^{-2}	f/kHz	PD/%	U/v	d_m/μm	w_m/μm	d_m/μm	w_m/μm
1	12	2	40	5	24.181	169.761	23.141	165.863
2	15	2	40	15	76.727	179.621	74.061	173.893
3	19	2	40	25	151.273	307.861	146.023	300.990
4	22	2	40	40	140.212	353.723	134.940	345.565
5	28	1.5	40	45	49.323	231.057	47.220	222.073
6	15	2	45	15	76.435	178.232	74.124	173.000
7	22	2	45	40	152.737	355.225	134.000	345.000

3.4. Experimental Verification

The stainless steel (SUS304) was selected as the material of micro-scaled flow channels during the ECM. And the input values of the neural network were used as the initial values of experimental parameters. The depth and width of flow channels under neural network prediction and electrochemical machining were compared and analyzed.

In this paper, the etching degree was introduced as the reference evaluation factor. The etching degree was defined as depth/width, which was used to further analyze the internal law of the ECM process of flow channels. After processing, the width, depth, and surface morphology of the workpiece were detected by SEM and Leica equipment, as shown in Figure 5 and 6.

With the increase of processing voltage, the average current density increased. The rate of material removal in-depth direction and width direction also increased. In this paper, it was evaluated by etching degree, as shown in Figure 4.

The SA-ANN prediction and experimental results showed that the voltage and current density had a significant effect on the depth and width of the flow channels. The etching degree generally increased with the processing voltage increased from 5V to 30V. The etching degree decreased slightly with the voltage was between 25V and 30V. It showed that when the voltage was from 25V to 30V, the machining voltage had little effect on the localization of the flow channel. The etching degree decreased rapidly with the voltage increased from 30V to 45V, which indicated that when the processing voltage was greater than 45V, the localization of ECM decreases rapidly. It means that too high voltage leads to too large width and too small depth of flow channel, which can not achieve the machining goal.

The prediction results of SA-ANN were consistent with the experimental results. Therefore, it was concluded that the voltage of the micro-scaled flow channel was selected between 15V and 30V, and 25V is the optimal parameter.

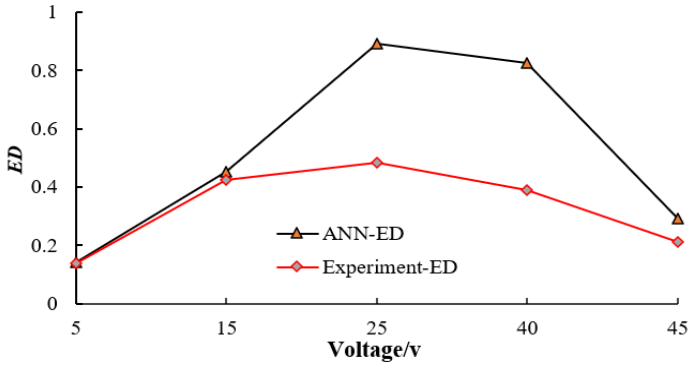

Figure 4. Variation Trend of etching degree under different voltages.

The morphology and cross-section in Figure 5 (a) are the results of the ECM of the flow channel when the voltage is 5V. The image shows that when the processing voltage is too small, the "island" shape will appear in the flow channel in the image, which will affect the forming of the channel. It means the processing voltage cannot be too small. The lateral etching of the channel was too fast with too large a processing voltage, which is easy to cause the disappearance of the "dam" between the channels. It finally led to the failure of channel processing. When the processing voltage was 45V, the morphology and section of the flow channel are shown in Figure 5 (b), the depth of the channel was 47.22μm, the width of the channel was 2×222.073μm, and the processing speed in the channel width direction was too fast to form a qualified flow channel.

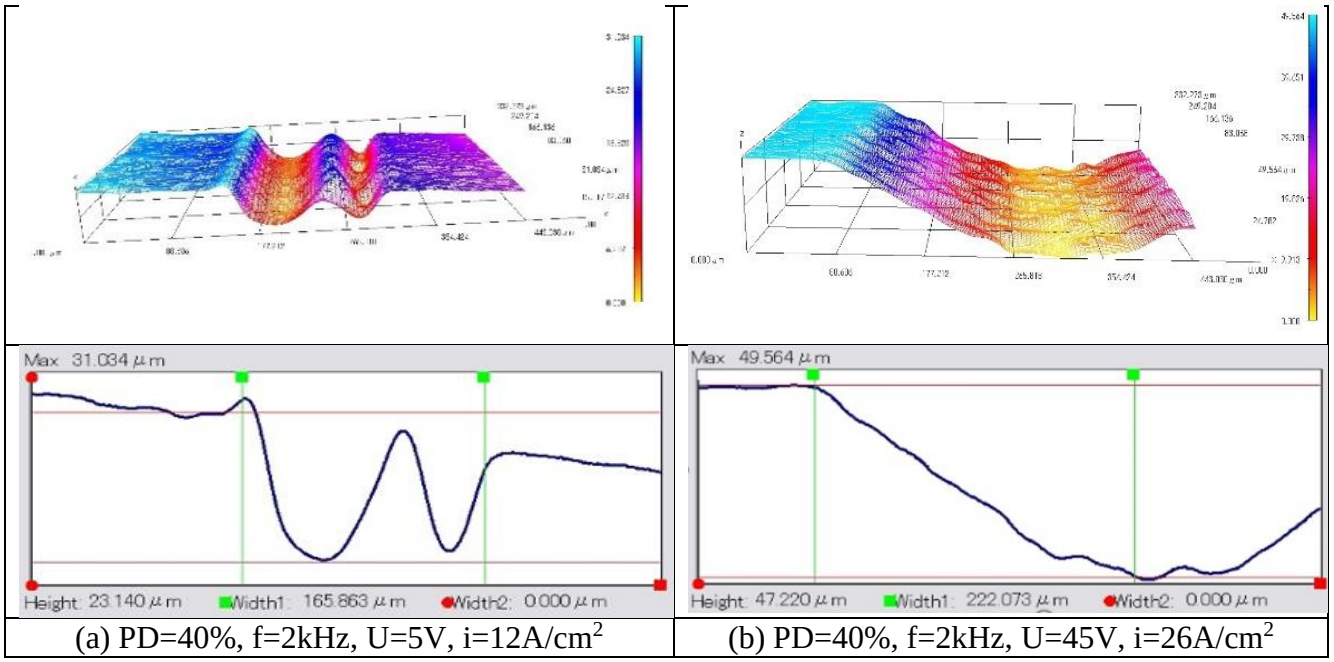

(a) PD=40%, f=2kHz, U=5V, i=12A/cm^2 (b) PD=40%, f=2kHz, U=45V, i=26A/cm^2

Figure 5. Morphology and section of channels.

The processing voltages selected in the experiment in Figure 6 are 15V, 25V, and 40V, and the average current densities are 15A/cm^2, 19.0A/cm^2, and 22A/cm^2. The morphology and cross-section of the channel are shown in Figure 6 (a) (b) (c).

The average current density was used in this research because of the use of a pulse power supply. The processing voltage increased from 5V to 25V, and the channel depth increased from 74.061μm to 146.023μm. The improvement rate of machining depth was 0.972, while the improvement rate of flow channel depth predicted by the artificial neural network was 0.97. Flow channel width increased from 173.893μm to 300.990μm. The improvement rate was 0.731, and the improvement rate predicted by the artificial neural network was 0.71. It showed that the ANN model could accurately predict the improvement rate of channel depth and width.

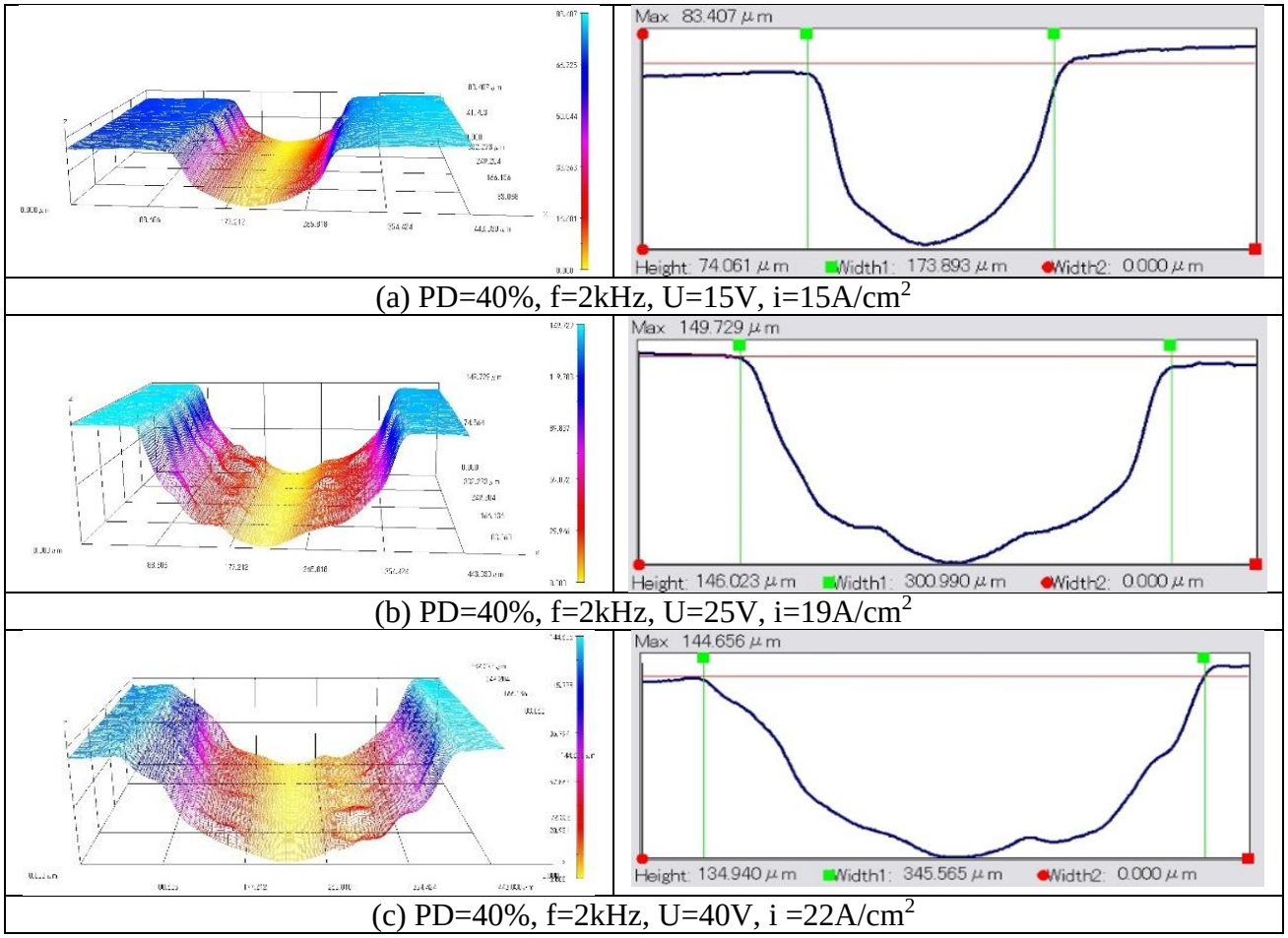

(a) PD=40%, f=2kHz, U=15V, i=15A/cm^2

(b) PD=40%, f=2kHz, U=25V, i=19A/cm^2

(c) PD=40%, f=2kHz, U=40V, i =22A/cm^2

Figure 6. Morphology and section of flow channels.

The etching degree of processing the test increased from 0.139 to 0.48, and the etching degree predicted by the SA-ANN model increased from 0.142 to 0.491. During the processing voltage from 25V to 40V, the etching degree decreased rapidly and an inflection point appears. If the processing voltage is too high, the channel width will be processed too fast and the depth will be too slow, which is not suitable for micro-scaled flow channel processing. It is concluded that the prediction ability of the

SA-ANN model constructed in this research met the requirements of optimizing parameters, which had excellent generalization ability. SA-ANN model can shorten the selection cycle of processing parameters and save experimental costs.

To sum up, the processing voltage is 25V, the current density is 19A/cm^2 and the pulse duty cycle is 0.4, which are the optimal parameter combination. The prediction results of the SA-ANN model and the morphology of the processing test can be confirmed.

After processing, the surface of the sample is shown in Figure 7. Figure 7 (a) is the morphology of the channel sample. Figure 7 (b) is the morphology of the channel after processing. Figure 7 (c) is the contour of the channel after processing.

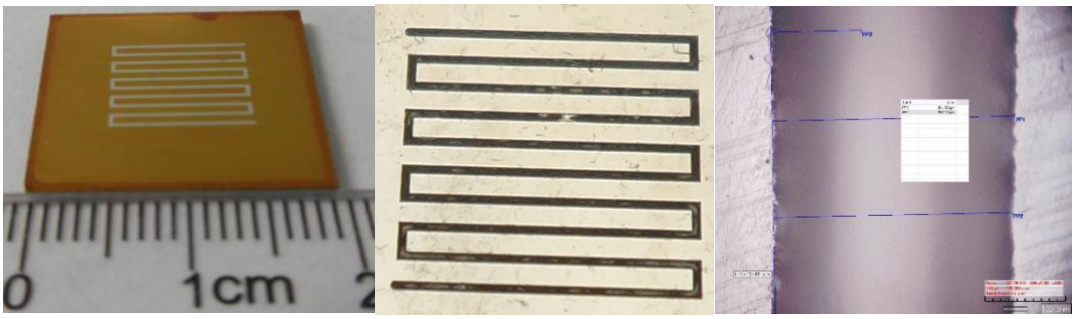

（a） （b） （c）

Figure 7. Topography of each stage of the channels.

4. CONCLUSIONS

In this paper, an artificial neural network based on simulated annealing was constructed to optimize the process parameters of micro-scaled flow channel ECM on the surface of stainless steel. The experimental data show that the SA-ANN has excellent prediction ability, and the prediction error is within 5.3%. It can reduce the parameter selection time of micro-scaled flow channels ECM, reduce the number of traditional orthogonal experiments and save experimental costs. It is noteworthy that the experimenters need to use the field data with strong pertinence in ECM to train the network model to achieve better results.

The prediction results of SA-ANN and experimental results show that the pulse current density and voltage have a great influence on the depth and width of stainless steel flow channels. Under the same voltage, the pulse duty cycle is between 0.2 and 0.4, and the influence coefficient of pulse on machining results is less than 0.007. Therefore, to improve the machining effect of stainless steel micro-scaled flow channel, voltage and current density are important.

Due to the small amount of experimental data of ECM examples, it is not suitable to use the currently popular deep neural network learning to predict ECM. In the follow-up work, the research team will make every effort to collect and mine the experimental data of various machining examples, find more factors affecting micro-scaled flow channel ECM, and pay attention to the progress of small data learning and prediction, as well as being committed to the improvement of the electrochemical machining process.

References

1. N. Smets, S. V. Damme, D. D. Wilde, G. Weyns, J. Deconinck, *J. Appl. Electrochem.*, 40.1(2010) 205.
2. V. Rathod, B. Doloi, B. Bhattacharyya, *Int. J. Pre. Technol*., 7(2017)169.
3. K. P. Rajurkar, M. M. Sundaram, A. P. Malshe, *Procedia CIRP*.,6(2013)13.
4. Aakash, S. S. Banwait, *Int. J. Innov. Technol & Exp. Eng*., 8(2019) 2683.
5. H. S. Farwaha, D. Deepak, GS. Brar, *J. Mech. Sci. Technol*., 34(2020)5063.
6. T. H. Tsai, M. Y. Lin, W. L. Huang, Sadhana-Acad P Eng S., 46(2021)1.
7. A. Malik, A. Manna, *J. Braz Soc. Mech. Sci. Eng*., 40(2018)1.
8. P. Antil, S.Singh, A. Manna. *Mater. Sci. Forum*., 928(2018)144.
9. M. Fang, Y. L. Chen, L. J. Jiang, Y. S. Su, Y. L. Liang, *Int. J. Adv. Manuf. Technol*., 105(2019)3261.
10. M. K. Das, K. Kumar, T. K. Barman, P. Sahoo, *Procedia Eng*., 97(2014)1587.
11. K. Vikas, D. K. Ashwani, *Int. J. Latest Trends. Eng & Technol*., 8 (2017)1.
12. G. B. Pang, D. M. Li, L. P. Zhang, Y. P. Peng, *Chin Mech Eng*.,24 (2013)1.
13. Z. Y. Li, H. Ji, H. L. Liu, *Adv. Mater. Res*., 121(2010)893.
14. W. J. Song, S. G. Choi, E. S. Lee, *J. Electrochem. Sci. Technol*.,10(2019)1.
15. D. K. Kasdekar, V. Parashar, C. Arya, *Mater. Today. Proc*., 5(2018)772.
16. Y. F. Lu, Z. Y. Wang, R. Xie, S. Liang, *J Mater Process Tech*., 3(2019)57.
17. M. Manoochehri, F. Kolahan, *Int J Adv Manuf Technol.*, 73(2014) 241.
18. F. Yuan, Y. Lin, *J. Human Settlements. West Chin*.,34(2019)9.
19. E. Weinan, S. Wojtowytsch, *Res Math Sci*., 8(2021)1.

© 2022 The Authors. Published by ESG (www.electrochemsci.org). This article is an open access article distributed under the terms and conditions of the Creative Commons Attribution license (http://creativecommons.org/licenses/by/4.0/).